FUNDAMENTAL RESEARCH

For. Sci. 62(2):154–165
http://dx.doi.org/10.5849/forsci.15-054

geospatial technologies

Linking the Depth-to-Water Topographic Index to Soil Moisture on Boreal Forest Sites in Alberta

Gabriel S. Oltean, Philip G. Comeau, and Barry White

The depth-to-water (DTW) index is defined as the cumulative slope along the least-cost pathway from any cell in the landscape to the nearest flow channel. The flow channel network is determined by the flow initiation area selected, allowing the representation of various geological and topographical attributes of the landscape. We used data from 125 plots across five locations in the boreal forest of Alberta, Canada, to evaluate the following: the relationships between soil attributes and DTW; the optimal flow initiation area; and models to map the spatial variation of soil properties. Soil moisture regime (SMR), drainage class, and depth-to-mottles were strongly related with DTW, whereas soil nutrient regime, organic matter thickness, soil texture, and coarse fragment content exhibited weak and inconsistent relationships with DTW. A flow initiation area of 2 ha yielded the best representation for SMR, drainage class, and depth-to-mottles. DTW, flow accumulation (FA) and local slope were combined in a linear model to estimate and map SMR, whereas only DTW and FA were used to model drainage and depth-to-mottles. These results suggest that the DTW index can capture soil properties closely influenced by the water table but cannot characterize site and soil factors, which are also determined by parent material, climate, and vegetation.

Keywords: soil nutrients, soil drainage, flow initiation area, digital elevation model, remote sensing

Site and soil properties interact with climate to define forest site productivity, a key input for sustainable forest management and conservation applications. Numerous studies have sought to establish the relationships among various soil properties and site productivity to overcome challenges associated with using tree height (e.g., site index) to characterize productivity (Bontemps and Bouriaud 2014). Several studies have indicated that soil moisture and nutrient regime are associated with the site indexes of Douglas-fir (Klinka and Carter 1990), western redcedar (Kayahara et al. 1997), trembling aspen (Chen et al. 2002), or white spruce (Wang and Klinka 1996). Other studies have also tested, with limited success, soil aeration (Gale et al. 1991), mineral soil pH, and the carbon/nitrogen ratio (Kayahara et al. 1995), or a water-holding capacity index that integrates coarse fragment content, depth of the B and C soil horizons, and textural classes (Ung et al. 2001). The potential applicability of these models would be greatly enhanced if such soil properties could be predicted from remotely sensed data.

Accurate digital elevation models (DEMs), which provide valuable information about terrain morphology, are becoming increasingly available for large forested areas. Because topography controls soil formation processes at a relatively fine scale (e.g., hillslope and subwatershed), DEMs can provide information at appropriate resolutions for mapping mesoscale variations in soil properties (Major 1951, Moore et al. 1991). The depth-to-water (DTW) index, proposed by Murphy et al. (2007), considers the effect of both the horizontal and vertical distance from any cell in the landscape to the nearest flow channel. The DTW and accessory data (i.e., flow accumulation and flow channel network) have been adopted by the Government of Alberta and are being used to guide forest operations for an area of approximately 30 million ha. Studies indicated the superiority of DTW over the frequently used topographic wetness index (TWI) (Beven and Kirkby 1979) for mapping wet areas in the boreal forest (Murphy et al. 2009) and also in the riparian forests of the tropical zone (Maillard and Alencar-Silva 2013). Because DEM resolution and landscape variations have a larger influence on TWI values, soil moisture regime (SMR) was more accurately predicted by DTW than TWI in a study from the boreal forest of Sweden (Ågren et al. 2014). Relationships between a suite of soil variables and DTW were also reported by Murphy et al. (2011), who noted that TWI can complement, at least in certain areas, the information

Manuscript received May 10, 2014; accepted December 14, 2015; published online January 28, 2016.

Affiliations: *Gabriel S. Oltean (oltean@ualberta.ca), Department of Renewable Resources, University of Alberta, Edmonton, AB, Canada. Philip G. Comeau (pcomeau@ualberta.ca), Department of Renewable Resources, University of Alberta. Barry White (barry.white@gov.ab.ca), Forest Management Branch, Alberta Agriculture and Forestry.*

Acknowledgments: *This project was funded by Alberta Agriculture and Forestry. Access to the research sites was granted by the WESBOGY Association and the geospatial data were provided by Jae Ogilvie of the University of New Brunswick. We gratefully acknowledge the assistance of Barbora Smerekova in the field and the reviewers for providing highly valuable comments on earlier versions of the article.*

provided by DTW. Simpler indices such as landscape position, potential solar radiation, and exposure have also been used in studies of vegetation gradients (Allen et al. 1991), whereas flow accumulation, local shape of the terrain and water-holding capacity were combined by Iverson et al. (1997) to derive an integrated moisture index used to map the composition and productivity of oak forests.

The ecological applications of DTW have not been extensively studied, but the large number of studies across a variety of landscapes in which the TWI has been tested stimulates more work on DTW. Moore et al. (1993) found that TWI and other terrain attributes (e.g., slope and profile curvature) explained up to 64% of the variation in A horizon depth, organic matter, extractable phosphorus, and texture. In contrast to previous studies that were conducted within homogeneous watersheds with strong topography, Seibert et al. (2007) reported significant associations between a series of physical and chemical soil properties and TWI in the flat landscape of the Swedish boreal forest. Their results showed the strongest correlations with variables measured in the organic horizon, suggesting that terrain morphology has a greater influence on soil surface processes than attributes of deeper horizons, which are more closely controlled by the parent material. Moreover, different algorithms for calculating TWI are better suited for particular landscapes and applications. TWI calculated using a more distributed flow-routing algorithm (e.g., FD8) worked better for locating forested wetlands (Lang et al. 2013) and other broad features (Kopecky and Cizkova 2010, Petroselli et al. 2013), whereas the determination of linear features (e.g., flow channels) is more consistent under algorithms with greater flow convergence (e.g., D8 and D) (Tarboton 1997, Sorensen et al. 2006).

In a similar manner, the delineation of flow channel networks, necessary to calculate DTW, is controlled by adjustment of the flow initiation area, allowing us to simulate general changes in soil moisture (e.g., wet or dry year and early or late season conditions). The general consensus is that a flow initiation area of 4 ha would be suitable to represent wetness conditions late in the season and stream channels with permanent or intermittent flow (White et al. 2012). Therefore, most studies have focused on this threshold (Murphy et al. 2009, 2011). However, Ågren et al. (2014) reported that the flow initiation area must be adjusted based on the hydraulic conductivity of the terrain. These results support further testing of different threshold values to evaluate the capabilities and limitations of the DTW index.

The availability of DTW rasters and the necessity to estimate key site and soil properties that influence productivity, silviculture, and harvesting in the boreal forest require a clear understanding of the limitations of DTW to predict these soil attributes. Furthermore, the effect of different flow initiation areas on the relationship between DTW and soil properties is not clearly understood, and optimal thresholds have not been proposed. The objectives of the study presented in this article were the following: to explore relationships between soil properties and DTW; to find an optimal flow initiation area; and to develop and demonstrate application of empirical models capable of mapping the spatial variation of soil attributes using only remotely sensed data. We hypothesize that DTW will show stronger associations with water-related soil properties than with other physical attributes (e.g., coarse fragment content and texture) and that a smaller flow initiation area will better capture the effects of topography on soil moisture.

Materials and Methods

Study Sites

Soil and site data were collected at five areas located in the Central Mixedwood natural subregion of the boreal forest of northern Alberta (Figure 1; Table 1). Four of these sites are part of a long-term study established between 1991 and 1992 by the Western Boreal Growth and Yield Association (WESBOGY) to study the development of aspen and spruce mixtures (Bokalo et al. 2007), whereas the Judy Creek (JC) research site was established in 2003 to evaluate selected strategies for establishment of intimate mixtures (Pitt et al. 2010). Glacial erosion has shaped the fine-textured glacial till deposits to define the geomorphology of the region. The parent material at JC is similar but presents a layer of rounded cobble at about 25–40 cm, indicating the effect of postglacial fluvial activity. The terrain of the areas studied has gentle slopes (0–10%) and elevational differences between the plots at one location ranging from 3 m at the Alberta Sustainable Resource Development (SRD) site (area of 16 ha) to 14 m at JC (area of 18 ha). This lack of strong topographic gradients reduces the control of relief on soil formation processes, thus decreasing the performance of topographic indices to predict soil attributes.

The climate of this area is characterized by long cold winters and warm summers: the mean annual temperature is 1.5° C and total precipitation is 389 mm; summer (i.e., May–August) has a mean temperature of 13.7° C and receives 60% of the total precipitation (Beckingham and Archibald 1996). The site at JC is the warmest (2.9° C) and receives the most precipitation (544 mm), whereas Daishowa-Marubeni International, Peace River (DMI_PR) is the driest (386 mm) and Daishowa-Marubeni International, Hines Creek (DMI_HC) has the lowest mean annual temperature (0° C). The majority of the soils developed in the five areas fall in the Great Group of Gray Luvisols, diagnosed by a clay accumulation horizon (i.e., Bt) with fine texture, although some soils are better developed with a higher pH and are classified as Eutric Brunisols. The woody vegetation of the Central Mixedwood subregion consists mainly of mixtures of white spruce (*Picea glauca* ([Moench] Voss) and trembling aspen (*Populus tremuloides* Michx.), but lodgepole pine (*Pinus contorta* Douglas) and black spruce (*Picea mariana* Mill.) can be found on drier raised sites and wetter depressions, respectively.

Field Survey

During the summer of 2013, 125 plots were sampled across the five study sites as shown in Table 1. The size of the plots assessed at the WESBOGY sites is 20 × 20 m with a 5-m buffer on each side, whereas 12 plots at JC are 35 × 35 m and the other 25 plots are 45 × 45 m. The geographic location of the plots was recorded with a Trimble GeoExplorer 6000 series GeoXT handheld device (Trimble, Los Altos, CA) with GNSS capabilities (the Global Navigation Satellite System combines the global positioning systems [GPS], GLONASS, and Galileo systems) that, under clear sky conditions, assured submeter accuracy. Site reconnaissance, identification of understory species composition, and the excavation of a soil pit were conducted according to the methodology described in Beckingham and Archibald (1996). Slope and aspect were measured using a clinometer and a compass, respectively, whereas the field guide was used to determine plant species composition. A soil pit limited by the C horizon (i.e., 55–90 cm) was dug in the center of each plot, and thickness of the organic matter, humus form, effective texture (i.e., texture of the finest textured horizon at least 10-cm thick located 20–60 cm

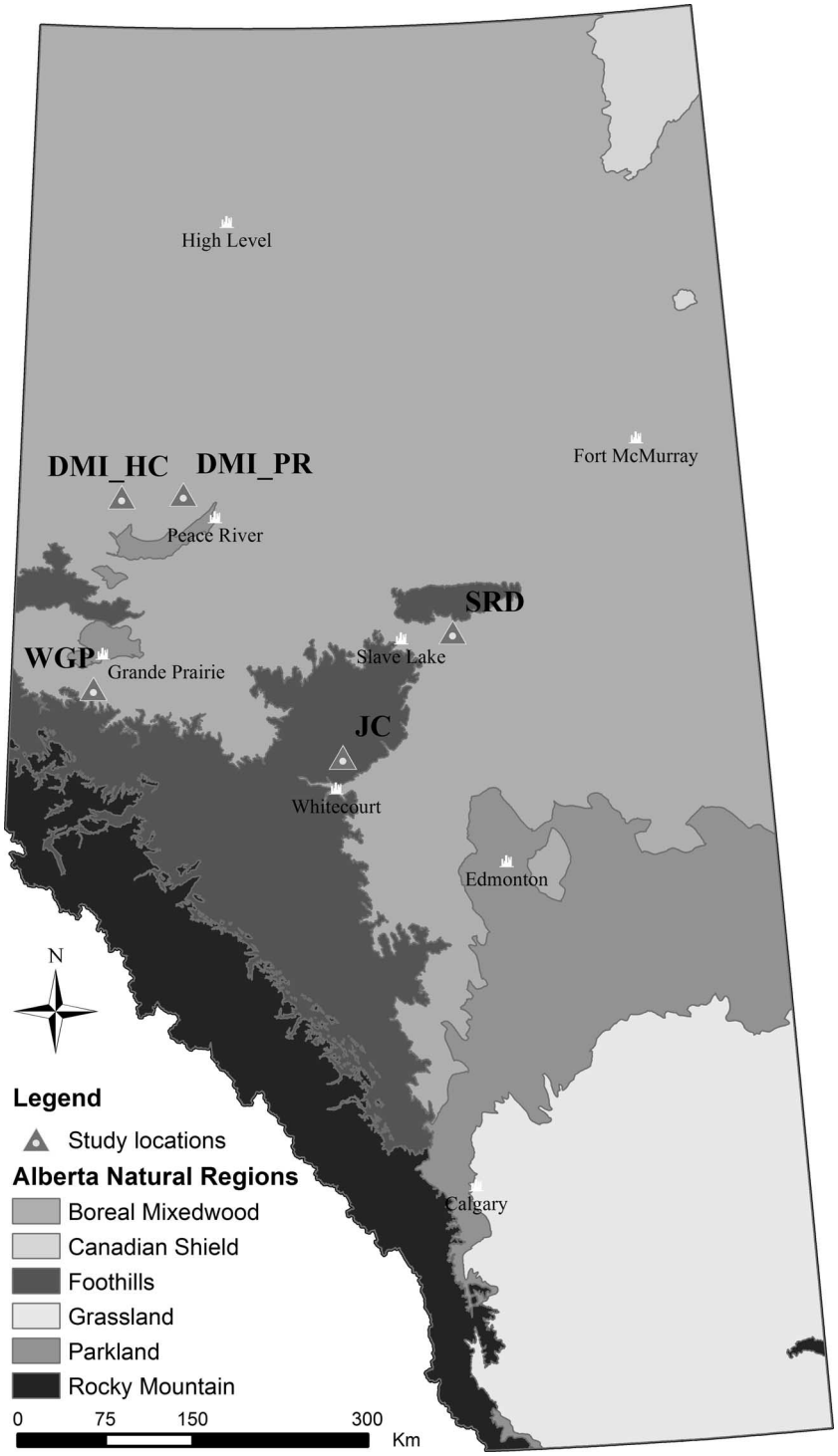

Figure 1. Location of the five study areas in the Boreal Mixedwood natural region of Alberta.

below the mineral soil surface), depth-to-mottles (DtMot), coarse fragment content and drainage class (imperfect, moderately well, and well) were determined. The drainage regime was determined based on features of the organic matter horizon and mottling layer together with texture of the mineral soil horizon.

Site-level information (i.e., topographic position, aspect, slope, and primary water source) was used together with information on effective texture, drainage class, and organic matter thickness to determine SMR and soil nutrient regime (SNR) as described by Beckingham and Archibald (1996). Thus, these measures of SMR and SNR integrate the spatial and temporal effects of all environmental variables that control moisture conditions and nutrient richness of the plots. The gradient of moisture regimes covered by our plots was limited to subhygric-mesic-submesic, sites most suitable for spruce-aspen mixedwoods. *Subhygric* sites were found on lower slight slopes that are receiving water from precipitation and through seepage and which are imperfectly to moderately well drained, favoring the accumulation of organic material. Sites on midslopes where precipitation is the main source of water and soils have better drainage with a thinner organic layer were considered *mesic*. Sites

Table 1. Summary of the geographic position and climate for the five study locations.

Location	No. of plots	Latitude (°N)	Longitude (°W)	Elevation (m)	MAT (° C)*	MST (° C)	MAP (mm/yr)	MSP (mm/summer)	Weather Canada station
JC	37	54.3826	115.6398	1,002.1	2.9	13.6	544.4	334.6	Whitecourt A
WGP	30	54.8864	118.9393	701.1	2.4	13.4	478.2	243.6	Grovedale RS
SRD	20	55.2982	114.0982	622.4	2.1	13.6	480.6	288.5	Slave Lake A
DMI_HC	18	56.3992	118.6029	795.7	0.0	12.6	436.2	251.4	Eureka River
DMI_PR	20	56.4071	117.7777	731.4	1.6	13.9	386.3	215.4	Peace River A

JC, Judy Creek; WGP, Weyerhaeuser Grande Prairie; SRD, Alberta Sustainable Resource Development (currently Alberta Agriculture and Forestry); DMI_HC, Daishowa-Marubeni International, Hines Creek; DMI_PR, Daishowa-Marubeni International, Peace River; MAT, mean annual temperature; MST, mean summer temperature; MAP, mean annual precipitation; MSP, mean summer precipitation (summer is defined as May–August).
* Data extracted from "1981–2010 Canadian Climate Normals" available at climate.weather.gc.ca.

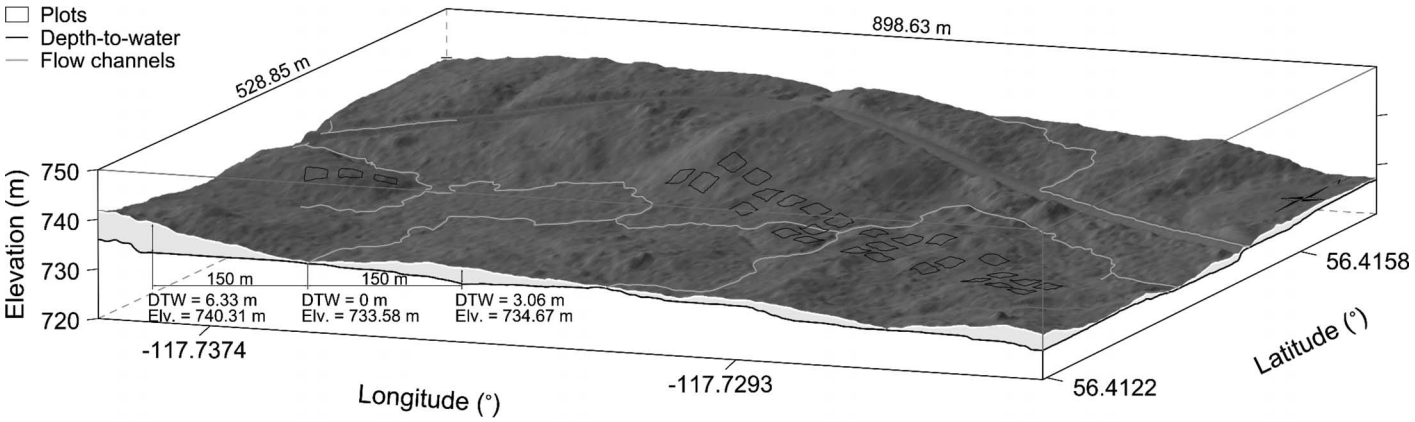

Figure 2. Perspective view and cross-section of the DMI_PR study site with the flow channels and DTW index calculated at 2 ha flow initiation area. The area of 47.5 ha has a minimum elevation of 725 m in the northeast corner and a maximum of 741 m in the southwest corner. See text (Algorithm for the DTW Index) for interpretation of the DTW values shown on the diagram.

located on upper slopes were defined as *submesic* and showed rapid drainage to well drained, and organic matter thickness was shallower.

Algorithm for the DTW Index

The DTW index, measured in meters, is the sum of slopes along the least-cost path from any cell in the landscape to the nearest flow channel, expressed as

$$\mathrm{DTW} = \left[\sum \frac{dz_i}{dx_i} a\right] x_c(m)$$

where dz_i and dx_i are the vertical and horizontal distance between two cells, respectively, a is a constant equal to 1 if the path that connects two cells is parallel to the cell boundaries and $\sqrt{2}$ if it connects the cells diagonally, and x_c is the size of the raster cell. Thus, a cell farther or at higher elevation from a flow channel will have a larger DTW value and is considered to be less hydrologically connected (i.e., it is drier) with the flow channel (Murphy et al. 2009).

The airborne light detection and raging (LiDAR) point cloud used to generate the DEM for the study sites had between 0.5 and 3 returns per m^2 with vertical accuracy of 30 cm at the 95% confidence interval. The 1-m resolution DEM was hydrologically conditioned to remove false depressions that obstruct water flow to determine flow direction based on the slope to the eight neighboring cells and flow accumulation (FA). The D8 single direction algorithm, which directs flow from each cell to one adjacent cell with the steepest downslope gradient (O'Callaghan and Mark 1984), was used because a dispersive flow direction algorithm (e.g., D∞) provides little improvement over D8 (Murphy et al. 2009). The FA value for a particular raster cell represents the number of 1 m^2 cells that divert flow to that cell, hence defining the area from which water is collected in any cell of the raster. Flow channels start in the cell for which FA meets the chosen threshold for the flow initiation area. We used threshold values of 0.5, 1, 2, 4, 8, 12, and 16 ha to define the flow channels based on which iterative function can calculate the DTW raster. To further illustrate the variation of the DTW index across the landscape, a diagram of the DMI_PR area shows the terrain and the DTW (belowground thick line) calculated at 2 ha flow initiation area is shown in Figure 2. Note that DTW is 0 m in the flow channels, and it integrates both horizontal and vertical distances from any cell to the flow channel; a cell located 1 m higher and 150 m away from a channel receives a DTW value of 3.06 m, whereas with the same horizontal distance but a 6-m difference in elevation the DTW value doubles to 6.33 m. The changes in DTW values induced by different flow initiation areas are illustrated in Figure 3.

Statistical Analysis

Linear mixed-effects models were used to explore the relationships between the response and the predictor variables, except for DtMot for which we used a nonlinear mixed model of the form $f(x) = ax^b$. The site and soil properties studied (SMR, drainage, DtMot, SNR, organic matter thickness, coarse fragment content, and effective texture) are continuous in their nature and, consequently, were treated as continuous dependent variables sampled from normally distributed populations. In the analysis of DtMot, we used only the plots where the mottling layer was found and the actual DtMot could be measured ($n = 72$). The average DTW, FA,

Table 2. Generalized coefficient of determination and statistical significance of the models that describe the relationships between soil properties and DTW calculated at different flow initiation areas, flow accumulation, and local slope.

	Flow initiation area used to calculate the DTW index							$\log_{10}$(FA)	Slope
	0.5 ha	1 ha	2 ha	4 ha	8 ha	12 ha	16 ha		
SMR									
$\bar{R}^2_{LR}$	0.09	0.14	0.16*	0.12	0.09	0.05	0.05	0.13	0.06
P value	0.0001	<0.0001	<0.0001*	<0.0001	0.0010	0.0275	0.0275	<0.0001	0.0069
Drainage regime									
$\bar{R}^2_{LR}$	0.15	0.19	0.30*	0.18	0.17	0.02	0.02	0.19	0.05
P value	<0.0001	<0.0001	<0.0001*	<0.0001	<0.0001	0.1311	0.1314	<0.0001	0.0231
DtMot									
$\bar{R}^2_{LR}$	0.28	0.17	0.42*	0.26	0.21	0.13	0.13	0.28	0.04
P value (*a*)	<0.0001	<0.0001	<0.0001*	<0.0001	<0.0001	<0.0001	<0.0001	<0.0001	<0.0001
P value (*b*)	<0.0001	0.0006	<0.0001*	0.0001	0.0001	0.0018	0.0018	<0.0001	0.0009
SNR									
$\bar{R}^2_{LR}$	0.06	0.06	0.01	0.02	0.02	0.02	0.02	0.09	0.02
P value	0.0218	0.0170	0.3511	0.2242	0.1912	0.1528	0.1543	0.0035	0.2273
Organic matter thickness									
$\bar{R}^2_{LR}$	0.00	0.00	0.01*	0.00	0.00	0.00	0.00	0.01	0.01
P value	0.4627	0.6286	0.2480*	0.9081	0.5453	0.4153	0.4144	0.4141	0.3489
Coarse fragment content									
$\bar{R}^2_{LR}$	0.00	0.00	0.00	0.02	0.04	0.08*	0.08	0.00	0.02
P value	0.9952	0.8821	0.4598	0.0978	0.0144	0.0004*	0.0004	0.5311	0.1684
Effective texture									
$\bar{R}^2_{LR}$	0.00	0.00	0.01	0.11*	0.10	0.07	0.07	0.02	0.01
P value	0.9685	0.8016	0.4185	0.0002*	0.0005	0.0025	0.0025	0.2169	0.2593

DtMot was modeled using a power function of the form $f(x) = ax^b$, and the associated *P* values for the two parameters are reported.
* Values showing the strongest relationships across the seven variants of DTW.

and slope were calculated and extracted for each of the 125 plots with ArcGIS 10.1 (ESRI, Redlands, CA) and used as independent variables to explain variation in the site and soil attributes. Logarithm in base 10 was applied to FA, and the transformed values were used in the analysis to ensure linear relationships.

The random factor in the mixed-effects model was considered to be the site location since the SRD site was generally drier and the Weyerhaeuser Grande Prairie (WGP) site was classified as the wettest, whereas the three other sites had both dry and wet plots. Likelihood ratio tests were used to select the optimal structure for the random effects. In the case of SMR, the intercept and slope were allowed to vary from site to site within a multiple of an identity variance-covariance matrix (Pinheiro and Bates 2000, p. 157–166) that constrains the random effects to be independent and have the same variance. A random effect was used on parameter a in the modeling of DtMot, whereas all of the other soil properties were modeled with a random intercept only. The structure of the random effects can be simplified when significant covariates enter the model (Pinheiro and Bates 1995); thus, the final models will either have different random-effects structures, as described in the section Modeling Significant Site and Soil Properties below or no random effects. Visual examination of the diagnostic plots for the final models revealed that the variance of the errors differed among locations; therefore, a variance function that calculates different weights for each study site was used. The variance parameter for one site was fixed at 1 for identifiability (Pinheiro and Bates 2000, p. 206–210). The structure of the variance function differed between models and it is presented below in Modeling Significant Site and Soil Properties.

The fixed-effects parameters, variance components, and functions were estimated using the restricted maximum likelihood method for the linear models, whereas the computational complexity of the nonlinear equation used for DtMot restricted us to the method of maximum likelihood. Thus, the traditional coefficient of determination (i.e., R^2) could not be used to assess the strength of the relationships and compare among models. Instead, we used a generalized R^2 defined as

$$R^2_{LR} = 1 - \left[\frac{L(0)}{L(\hat{\beta})}\right]^{\frac{2}{n}} = - \exp\left\{-\frac{2}{n}[l(\hat{\beta}) - l(0)]\right\},$$

where n is the sample size, and $l(0) = \log L(0)$ and $l(\hat{\beta}) = \log L(\hat{\beta})$ represent the log-likelihood of the null and the fitted model, respectively (Maddala 1983, p. 37–41, Cox and Snell 1989, p. 208–209, Magee 1990). This measure of fit (i.e., R^2_{LR}) is consistent with classic R^2 defined in the context of simple linear regression, but it fails to achieve the maximum of 1 for models where the likelihood is calculated as a product of probabilities. Nagelkerke (1991) calculates this maximum for R^2_{LR} and proposes the following definition

$$\bar{R}^2_{LR} = \frac{R^2_{LR}}{\max(R^2_{LR})}$$

$$\text{where } \max(R^2_{LR}) = 1 - L(0)^{\frac{2}{n}} = 1 - \exp\left\{\frac{2}{n}l(0)\right\}.$$

To compare the predictive power of the DTW index calculated at the seven flow initiation areas, the $\bar{R}^2_{LR}$ values in Table 2 were calculated against a null model that included the same random effect structure to ensure that it reflects only the additional model improvement given by the fixed effect. The $\bar{R}^2_{LR}$ values reported for the final models in Modeling Significant Site and Soil Properties below and Table 3 were calculated using a simple mean model with no random effects.

The covariates and their interactions included in the final models were selected based on conditional or Wald-type *t*-tests and model

Table 3. Estimates of the fixed effects, variance components (as SDs), variance parameters, and residual variances (as SDs) with the associated 95% CIs for Equations 1, 2, and 3.

Fixed effect	Estimated coefficient (95% CI)	*P* value	Variance function/random effect	Estimated parameter (95% CI)
SMR ($\bar{R}^2_{LR} = 0.43$)				
β_0 (intercept)	5.277 (4.896 to 5.658)	<0.0001	δ_1 (DMI_HC)	1 (set value)
β_1 (DTW)	−0.141 (−0.209 to −0.074)	0.0001	δ_2 (DMI_PR, SRD)	0.760 (0.499–1.157)
β_2 [$\log_{10}$(FA)]	0.295 (0.168 to 0.422)	<0.0001	δ_3 (JC, WGP)	1.272 (0.867–1.868)
β_3 (slope)	−0.078 (−0.131 to −0.024)	0.0052	Residual SD (σ)	0.412 (0.293–0.581)
Drainage class ($\bar{R}^2_{LR} = 0.62$)				
β_0 (intercept)	3.501 (3.099 to 3.902)	<0.0001	δ_1 (SRD)	1 (set value)
β_1 (DTW)	−0.235 (−0.308 to −0.162)	<0.0001	δ_2 (DMI_HC, DMI_PR)	1.686 (1.132–2.513)
β_2 [$\log_{10}$(FA)]	0.347 (0.209 to 0.485)	<0.0001	δ_3 (JC, WGP)	3.154 (2.192–4.539)
			Random effect SD (σ_b)	0.200 (0.084–0.476)
			Residual SD (σ)	0.214 (0.156–0.296)
DtMot ($\bar{R}^2_{LR} = 0.63$)				
β_{a0} (a intercept)	40.037 (32.939 to 47.134)	<0.0001		
β_{a1} [$a \log_{10}$(FA)]	−5.661 (−8.673 to −2.648)	0.0004		
β_{b0} (b intercept)	0.557 (0.309 to 0.805)	<0.0001		
β_{b1} [$b \log_{10}$(FA)]	−0.120 (−0.235 to −0.005)	0.0418	Residual SD (σ)	7.502 (6.426–9.015)

Results from conditional significance tests of the fixed effects and the generalized coefficient of determination ($\bar{R}^2_{LR}$) are shown for each model.

parsimony was ensured using Akaike weights. Multicollinearity was avoided because there was not a clear pattern between DTW and FA or slope, and the correlation coefficients were relatively low [DTW versus $\log_{10}$(FA): $r = -0.39$; DTW versus slope: $r = 0.40$; $\log_{10}$(FA) versus slope: $r = -0.18$]. The validity of the normality assumption on the errors was confirmed by visual examination of Q-Q plots and formal hypothesis testing with the Shapiro-Wilk test. Semivariograms revealed that the spatial correlation structure initially found in the residuals was successfully removed with the final models, therefore avoiding inflation of type I error. All mixed-effects models were fit using version 3.1-117 of the nlme library (Pinheiro and Bates 2000, Pinheiro et al. 2015) implemented in the R environment, version 3.1.0 (R Core Team 2015). A significance level of $\alpha = 0.05$ was used for all statistical tests.

Results

Site and Soil Properties in Relation to Terrain Attributes

SMR, drainage class, and DtMot were the site and soil attributes most strongly ($\bar{R}^2_{LR} = >0.16$) and significantly ($P < 0.0001$) associated with plot averages of DTW, FA, and slope, whereas SNR, the thickness of the organic layer, the percentage of coarse fragments, and effective texture did not show strong relationships ($\bar{R}^2_{LR} = <0.11$) with any of the topographic characteristics (Table 2). Soil wetness, as described by SMR, drainage, and DtMot, was negatively related to DTW (Figure 4) and terrain slope, whereas FA showed the opposite trend (i.e., plots with large FA were wetter). Average DTW (calculated at 2 ha) values of 1.10, 2.29 and 4.45 m corresponded to subhygric, mesic, and submesic conditions, respectively. Higher DTW values were significantly associated with moder humus, whereas raw moder humus was found at plots with lower DTW. Plots characterized with poor SNR were found at lower DTW, whereas medium and rich plots were associated with higher DTW values. No clear pattern was found between organic matter thickness, coarse fragment content, or effective texture and any of the terrain attributes.

Finding the Optimal Flow Initiation Area

DTW calculated at a flow initiation area of 2 ha was the strongest predictor of SMR, drainage class, and DtMot. However, threshold areas of 1, 2, 4, or 12 ha showed limited degrees of association with the other soil properties (Table 2, asterisks). When the flow initiation area was lowered or increased from 2 ha, the relationships between DTW and SMR, drainage, and DtMot became weaker or did not show significant and consistent patterns. The spatial effect of changing the flow initiation area is shown in Figure 3 in which one can note that at 0.5 ha a dense channel network is constructed ($L_{channels} = 6{,}445.7$ m) and consequently a larger area has low DTW values ($A_{DTW<1} = 29.3$ ha of the 47.5 ha), whereas at 16 ha only 1,857.4 m of flow channels are delineated with only 12.49 ha of <1 m. An intermediate threshold area of 2 ha identifies a channel network of 3,458.4 m with 19.7 ha of <1 m DTW. Threshold areas of 12 and 16 ha yield similar results both spatially (Figure 3) and statistically (Table 2).

Although statistically significant, the relationships between DTW at different flow initiation areas and the other soil characteristics are not strong ($\bar{R}^2_{LR} = <0.11$) and the pattern of gradual decrease in $\bar{R}^2_{LR}$ cannot be observed. Moreover, visual assessments of scatterplots revealed that the linear relationships between these soil properties and DTW are either driven by a few points or even change slope direction at different flow initiation thresholds.

Modeling Significant Site and Soil Properties

SMR was initially modeled linearly with DTW, calculated at a flow initiation area of 2 ha, as a fixed effect and random intercept and slope by location. Once $\log_{10}$(FA) and slope were introduced, the random effects did not contribute significantly to the model and were consequently dropped from the model. Because the variances of SRD and DMI_PR as well as those of JC and WGP were similar, these sites were aggregated into two groups, and the variance parameter of DMI_HC was set to 1. The final equation was of the form

$$SMR_{ij} = \beta_0 + \beta_1 DTW_{ij} + \beta_2 \log_{10}(FA_{ij}) + \beta_3 Slope_{ij} + \varepsilon_{j(i)} \quad (1)$$

where SMR_{ij} is the observation in the jth plot nested in location i, and β_0, β_1, β_2, and β_3 represent the intercept and coefficients of DTW, FA, and slope, respectively. The errors are assumed to be independent and identically distributed (i.i.d.) as $\varepsilon_{ij} \sim N(0, \sigma^2\delta_i^2)$, where σ^2 is the error variance and δ_i is the variance parameter. This model provided an $\bar{R}^2_{LR}$ of 0.43 against a simple

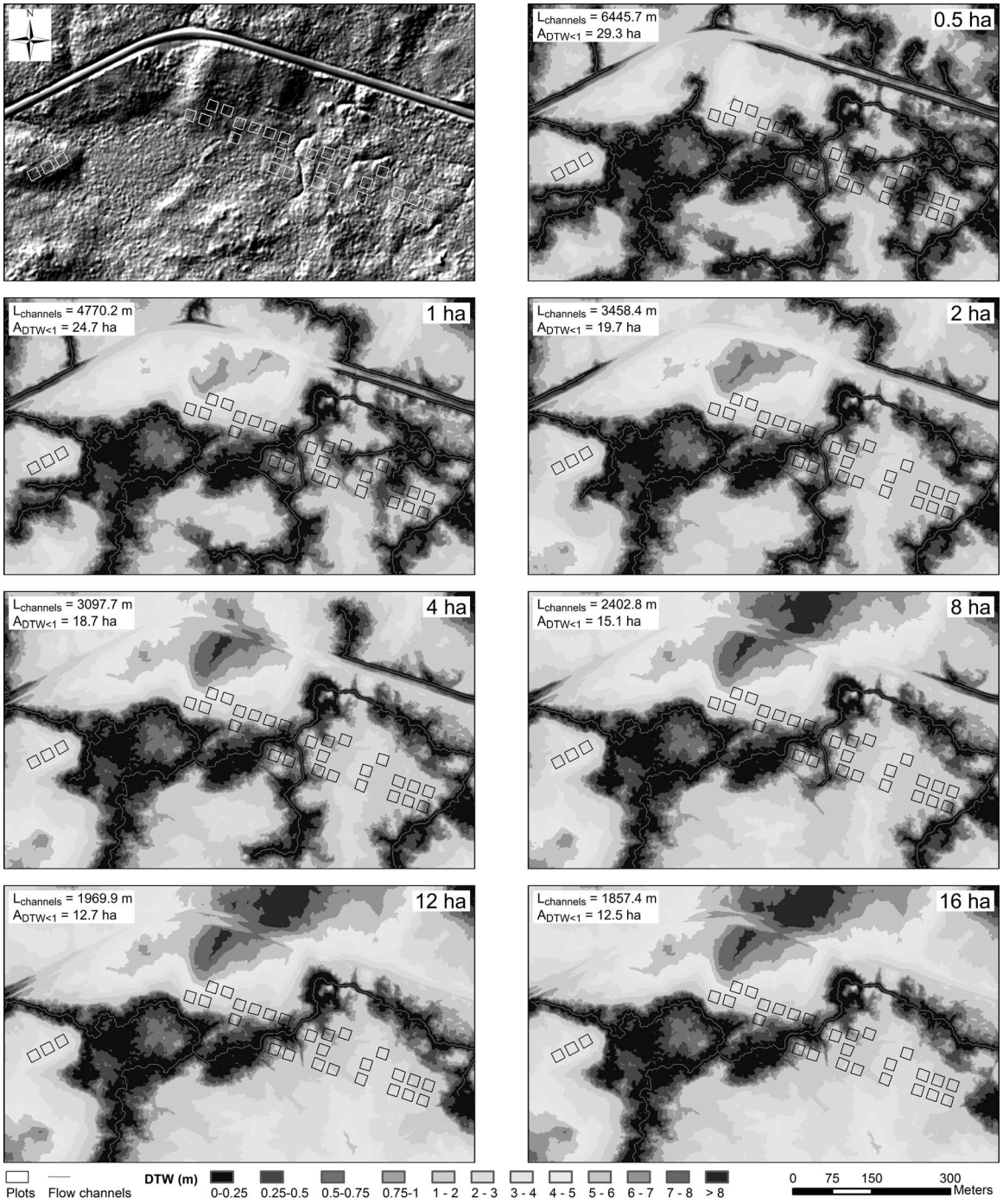

Figure 3. The DTW raster and flow channels calculated at flow initiation areas of 0.5, 1, 2, 4, 8, 12, and 16 ha illustrated for the DMI_PR study site. The top-left image represents a hillshade view of the DEM raster to facilitate identification of landscape features (e.g., raised and low-lying areas and the road). The 20 × 20-m rectangles are the 30 plots established at this WESBOGY site. $L_{channels}$, length of the flow channels identified in the area; $A_{DTW<1}$, area of terrain with DTW < 1 m.

mean model and was exemplified for the DMI_PR location to produce the map in Figure 5.

Drainage regime was at first modeled as a function of DTW at 2 ha with a location-level random effect on the intercept. Adding $\log_{10}$(FA) to the model significantly increased the value of the likelihood function but did not affect the significance of the random effect, whereas slope did not improve the fit of the model significantly ($P = 0.1627$) and hence was not included. The variance parameter of SRD was set to 1, whereas DMI_HC was grouped with DMI_PR and JC with WGP. This model was described by the following equation

$$\text{Drainage}_{ij} = (\beta_0 + b_1) + \beta_1 \text{DTW}_{ij} + \beta_2 \log_{10}(\text{FA}_{ij}) + \varepsilon_{j(i)} \quad (2)$$

where Drainage_{ij} is the jth observation at location i and β_0, β_1, and β_2 indicate the intercept and coefficients of DTW and FA, respectively. The random effects b_i are assumed to be normally distributed as

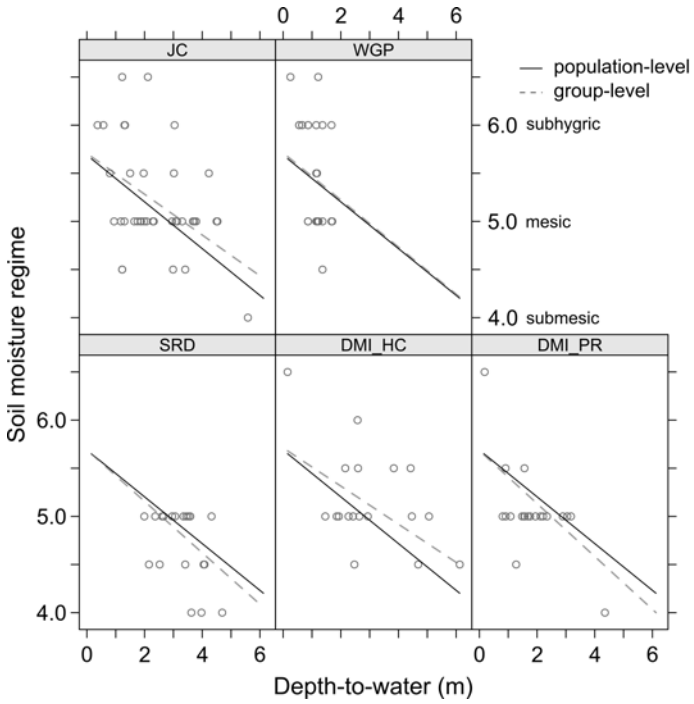

Figure 4. SMR in relation to DTW calculated using a flow initiation area of 2 ha shown by location. The solid line represents the population-average model, and the dashed line illustrates how the random effect for the intercept and slope affects the linear model parameters at each location.

$b_i \sim N(0, \sigma_i^2)$, where σ_i^2 is the variance component, and the residuals to be i.i.d. as $\varepsilon_{ij} \sim N(0, \sigma^2\delta_i^2)$, where σ^2 is the error variance and δ_i is the variance parameter. An $\bar{R}^2_{LR}$ of 0.62 was obtained for this model, which is illustrated in Figure 6.

To model DtMot, we used a power function of the form $f(x) = ax^b$, where x was DTW at 2 ha and a random effect was allowed on parameter a. Subsequently, the estimated best linear unbiased predictors (i.e., estimated location-level random effects) were linearly related with $\log_{10}$(FA) and the random effect was dropped. Slope did not explain the variation in DtMot. A variance function was not required. The resulting equation was

$$\mathrm{DtMot}_{ij} = [\beta_{a0} + \beta_{a1}\log_{10}(\mathrm{FA}_{ij})] \cdot \mathrm{DTW}^{[\beta_{b0}+\beta_{b1}\log_{10}(\mathrm{FA}_{ij})]} + \varepsilon_{j(i)} \quad (3)$$

where DtMot_{ij} is the jth measurement at study site i, β_{a0} and β_{a1} are the intercept and slope used to derive parameter a, and β_{b0} and β_{b1} are the intercept and slope needed to calculate parameter b of the power function. The error terms were assumed to be i.i.d. and $\varepsilon_{ij} \sim N(0, \sigma^2)$, where σ^2 is the variance of the residuals. The $\bar{R}^2_{LR}$ yielded from this model was 0.63, with Figure 7 showing the surface generated by it.

Discussion

Site and Soil Properties in Relation to Terrain Attributes

The general assumption behind the concept of topographic indices is that terrain morphology influences soil formation processes through its control of the accumulation and distribution of organic and mineral matter (i.e., slope) and exposure to the effects of weather phenomena (i.e., aspect). Further, topography has strong effects on the gravitational movement of water on and in the soil, which will influence pedogenesis and soil properties (Jenny 1941, p. 11–12, Major 1951). However, topography is only one component of the five soil-forming factors; thus, the accuracy of predictions for soil attributes based solely on relief is limited. Our first objective was to explore the relationships between DTW and a set of general site and soil characteristics based on the hypothesis that water-related soil attributes will show stronger association with the remotely sensed DTW index.

Expected relationships were found between DTW, SMR, drainage class, and DtMot (Table 2), which supports our hypothesis and agrees with previous findings. DTW has been linked directly to soil wetness (Ågren et al. 2014) and explained 64% of variation in soil drainage (Murphy et al. 2011) and indirectly through a vegetation index (Hiltz et al. 2012), which integrates soil properties, with an R^2 of 0.68. However, these studies used data collected from sites with more pronounced topography than ours, providing a wider range of soil characteristics and environmental conditions in terms of climate parameters and vegetation. For example, Murphy et al. (2011) were able to sample the entire range of moisture (i.e., hydric to subxeric) and drainage (i.e., very poor to rapid) conditions. Our study was conducted in the Central Mixedwood natural subregion of the boreal forest, on sites without large landscape features (e.g., valley or hill) that accentuate the control of topography on soil properties and create strong environmental gradients. Further, slopes ranged from 2.6 to 9.6% with a median of 4.5%; thus, the gravitational movement of water in and on the surface of the ground is not strongly influenced by terrain. Despite these limitations, our results suggest that DTW values (calculated at 2 ha) between 1 and 5 m can describe 43% of the variance in subhygric to submesic soil conditions, whereas wetter (i.e., hygric to hydric) or drier (i.e., xeric) sites must be captured by DTW values of <1 and >5 m, respectively.

Because topography alone does not control SNR, organic matter thickness, coarse fragment content, and texture, DTW did not relate strongly and predictably with these soil attributes. Moreover, the low relief of this landscape together with the strong influence of other pedogenetic factors (i.e., parent material, climate, and biota) make these soil attributes less predictable from terrain information only. Similarly, Ziadat (2005) reported weak or no associations between the texture or water-holding capacity of soils and terrain attributes on a large and flat (i.e., 1–4%) area in Jordan with topography similar to that of the boreal landscape. However, dividing the large areas into homogeneous landscape facets made soil-topography relationships more obvious and easier to prove statistically (Ziadat 2005). Although decomposition rates are closely related to water table levels, we did not find a strong association of DTW with organic matter thickness, in contrast to Murphy et al. (2011), who were able to establish a relationship between forest floor depth and DTW. This could be partly explained by the influence of other factors (e.g., vegetation and climate) on decomposition of organic matter and the wide range (i.e., 1–65 cm) of forest floor depths sampled by Murphy et al. (2011) compared with our data that spanned a range of only 3 to 15 cm. The weak to nonexistent associations between texture or coarse fragment content of the soil and DTW may be explained by the strong influence of the parent material and the weathering processes controlled by climate on these physical soil attributes. Further, the lack of steep slopes that can control the distribution of coarse fragments and the thickness of certain soil horizons (e.g., through erosion rates) (Daniel et al. 1979,

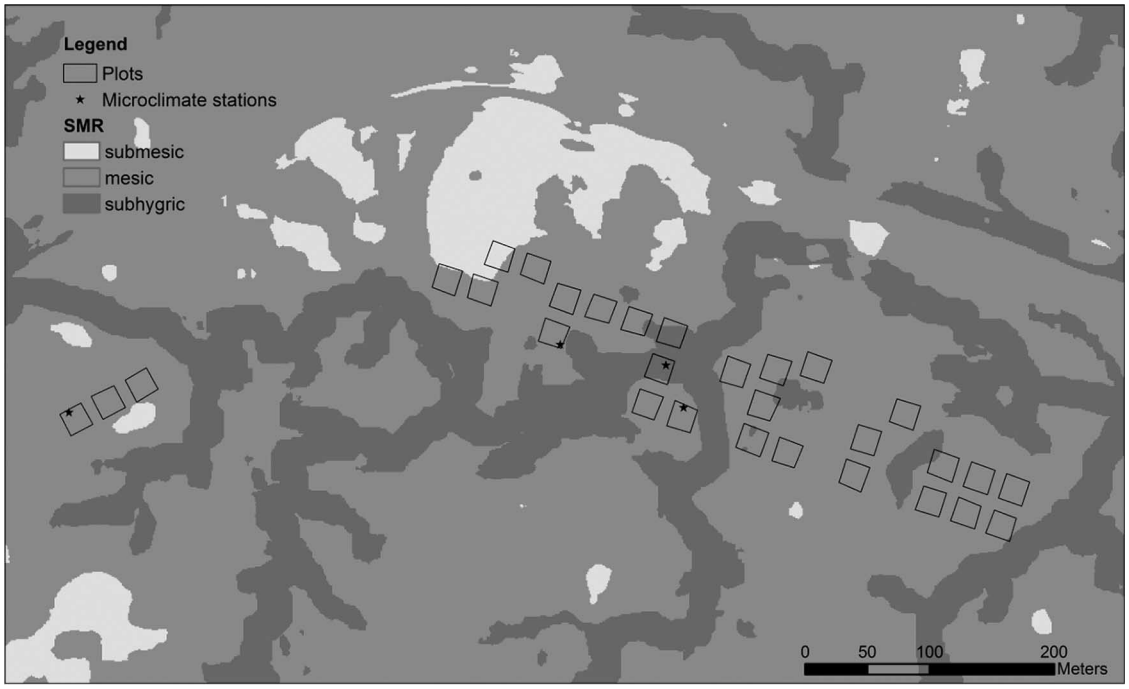

Figure 5. Map of the DMI_PR area showing the SMR calculated using Equation 1.

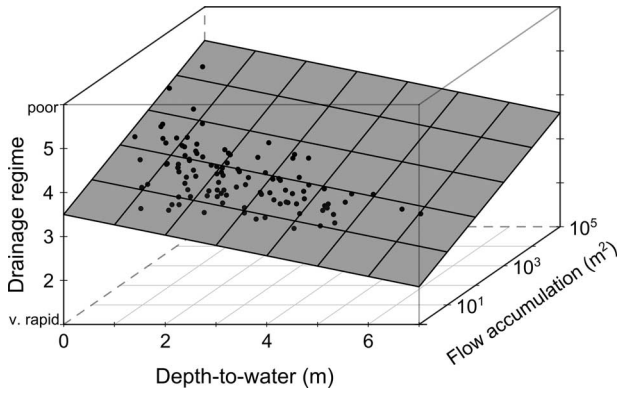

Figure 6. The geometric plane that illustrates the relationship between drainage regime, DTW calculated at 2 ha flow initiation area, and flow accumulation as defined by Equation 2. Note that the points on the plot are the fitted values and not the raw observations.

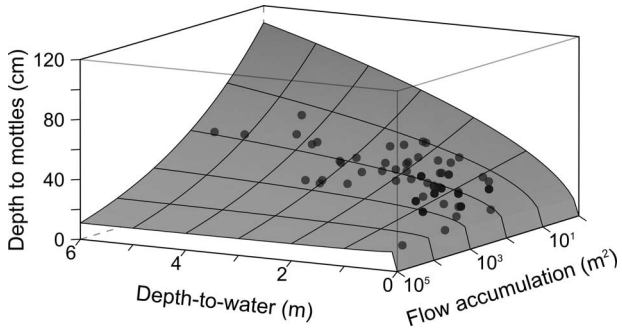

Figure 7. The shaded surface indicates the relationship between DtMot, DTW calculated at flow initiation are of 2 ha, and flow accumulation as determined by Equation 3. Note that the points on the graph are the fitted values.

p. 186–187) reduces the connection between topography and these soil characteristics.

Finding the Optimal Flow Initiation Area

The algorithm that calculates the DTW values for a cell in the landscape requires the identification of flow channels. The delineation of these terrain features starts at a certain threshold value (i.e., the flow initiation area) of the FA raster and follows the cells into which most of the neighboring cells drain the runoff and infiltrated water. As flow initiation thresholds decrease, flow channels extend further into the headwaters of the watershed and thus DTW values become smaller because the horizontal and vertical distance from any cell in the landscape to the nearest flow channel is decreased. On the other hand, large flow initiation thresholds will only identify the major streams of the basin (i.e., these collect water drained from larger areas), thus generating larger DTW values, especially in the upper zone of the watershed. The modeling of the spatial and temporal variation of the stream network and adjacent wet areas can be improved by changing the flow initiation area, with lower threshold values being used for wetter years, whereas larger thresholds can represent soil conditions during drier seasons (Ågren et al. 2014). A threshold area of 4 ha, for example, represents conditions frequently occurring late in the season in Alberta (White et al. 2012) and generates a network of channels corresponding to field-mapped ephemeral streams (Murphy et al. 2011).

We found that a flow initiation area of 2 ha provides the strongest relationships with SMR, drainage class and DtMot (Table 2). DTW calculated at threshold values of 1 and 4 ha also yielded strong relationships, a range that is consistent with the findings of Ågren et al. (2014) who reported that a threshold value of 1–2 ha yields the best results when soil wetness is mapped in a landscape whose geology consists of glacial till, characterized by low permeability. The same authors found that larger flow initiation areas (i.e., 10–16 ha) performed better in an area with high hydraulic conductivity given

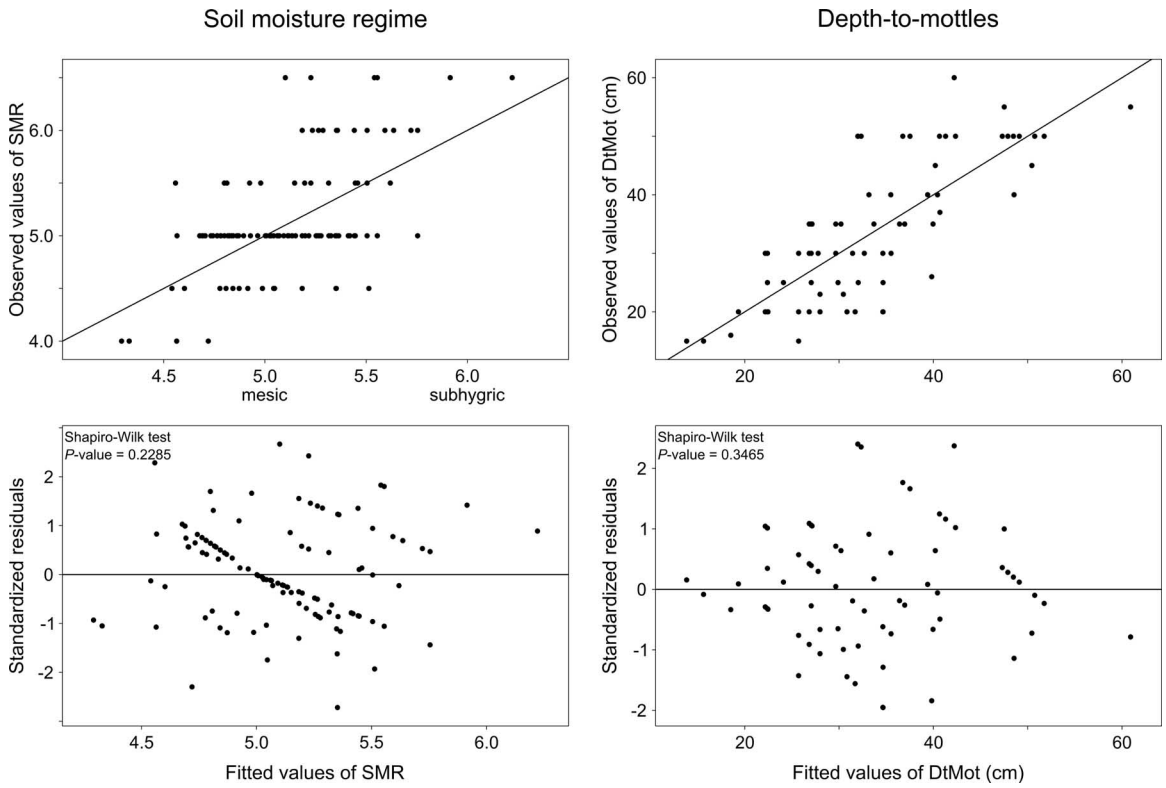

Figure 8. Observed versus fitted values of SMR (top-left panel) and DtMot (top-right panel), where the solid line shows the 1:1 relation, and standardized residuals against fitted values of SMR (bottom-left panel) and DtMot (bottom-right panel).

by the different geology (i.e., ice-river alluvium). A smaller catchment area was also recommended for predicting drainage and vegetation class (Murphy et al. 2011), but in this study the smallest threshold area used was limited to 4 ha (they also tested 5 and 6 ha) which does not exclude the possibility that smaller areas would have offered better results. A similar result was found when DTW calculated at 1 ha outperformed a threshold value of 4 ha in predicting the location of ruts in the boreal forest (Campbell et al. 2013). The results found for SNR, organic matter, coarse fragment content, and texture are weak and do not follow expected trends; thus, no conclusion can be made about the optimal threshold area for these parameters.

The site descriptors we used (i.e., SMR and drainage class) integrate site and soil factors at different scales (e.g., topographic position, slope gradient, ground vegetation, effective texture, and organic material thickness) representing average long-term conditions found at the plots. However, this does not eliminate the flexibility of adapting the DTW index to particular weather conditions (e.g., very dry or wet) by changing the flow initiation area, especially for operational applications (e.g., harvesting) when the extent of wet areas with soft ground that need to be avoided must be carefully delineated (White et al. 2012). Moreover, different threshold values can be used to adapt the DTW index to potential applications requested by various stakeholders (e.g., identification of protected wet areas and prediction of areas prone to flooding).

Modeling Significant Site and Soil Properties

Our third objective was to integrate remotely sensed topographic variables into empirical models that could be used to map the spatial variation of water-related soil attributes in the boreal forest. The final equation proposed for the SMR model includes DTW, FA, and slope (Equation 1; Table 3). In this model, DTW and slope are negatively influencing the SMR value, whereas higher FA values will increase the wetness of the site. For each raster cell, DTW provides information about hydrologic connectivity with flow channels, whereas FA indicates water supply from the upslope area, which is then corrected by the terrain slope. The use of a variance function to account for the heterogeneity of the error variance across the five locations indicates that sites with more uniform topographic conditions (e.g., DMI_HC and WGP) naturally create a narrower range of SMR, whereas a diverse landscape allows for a wider spectrum of soil conditions to develop. The scatterplot (Figure 8) of observed versus fitted values shows some departures from the 1:1 relationship on both sides of the SMR spectrum, indicating that the model tends to pull wetter and drier plots closer to mesic conditions. This could be an artifact of the large influence exerted by the greater number of observations for mesic SMR, which are spread across a relatively wide range of DTW overlapping with submesic and subhygric DTW values.

Similar to our model, Gessler et al. (2000) used TWI, FA, and slope to model the thickness of the A horizon and concluded that short-term processes are not captured by landform indices because these processes are more random and variable. This argument cannot be used to explain the weak fit of our SMR model because SMR integrates site and soil factors to provide long-term average soil conditions at the plots. However, Murphy et al. (2011) showed that DTW and soil depth can account for 68% of variation in a more specific measure of soil moisture (i.e., water-filled pore space), indicating that DTW cannot capture the totality of phenomena integrated by SMR. Based on our field observation, we can confirm the deficiency of Equation 1 noted in the 1:1 scatterplot (Figure 8) because the actual spatial extent of subhygric and submesic areas is

larger than that portrayed in Figure 5, where we applied the SMR model to the DMI_PR location. This lack of fit also suggests that Equation 1 may not follow a linear function and that it might be useful to incorporate additional variables (e.g., soil texture) other than terrain attributes to improve the predictive power of the model. However, we were not able to explore these alternatives because our data would not support a nonlinear relationship and other soil properties (e.g., soil texture) were not available at a resolution comparable to that of our study.

The final equation to model drainage (Figure 6; Equation 2; Table 3) consists of a positive relation with DTW and a negative coefficient for FA, indicating that areas with low DTW and high FA values drain more poorly, whereas actively drained sites will be found in zones farther away from flow channels. Local slope is not included in the model because it does not have a large influence on the drainage of the soils at our study areas, since their fine texture exerts a stronger control on water movement, especially under saturated conditions (Kimmins 2004, p. 291–292). This claim is supported by the necessity to use random effects to account for variation in drainage across the five study sites because of differences in soil texture. The negative conditional modes of the random effects (i.e., EBLUPS) for DMI_PR, SRD, and JC indicate that these sites were more actively drained, which is consistent with the lighter texture of these soils. On the other hand, the fine texture of soils at DMI_HC and WGP was accounted for in the model with the random effect. Because our objective was to use remotely sensed indices to predict site and soil properties, we did not include field-assessed texture in the model. This limitation is also visible in the scatterplot of observed versus fitted values, which shows a slight tendency of Equation 2 to overestimate drainage of imperfectly drained soils.S

We used a power function to model the functional relationship between DtMot and DTW because it provided a better fit than a linear function, and we do not expect DtMot to be bound by an asymptote. If data from soil pits where mottles were not found was grouped in a class labeled ">50 cm," then a sigmoidal curve would have been favored, but this functional form is not acceptable because the DtMot is not limited to an arbitrary depth of 50 cm. The final form of the model (Equation 3; Table 3) uses DTW as the driving variable, whereas parameters a and b are negatively dependent on FA, indicating that cells collecting water from a larger area are more likely to undergo mottling (Figure 7). The process of soil mottling is directly dependent on fluctuations in the level of the water table, thus the good agreement between the observed and fitted values was to be expected (Figure 8). The strong connection between mottling and depth to the water table was also reflected in Equation 3, which yielded the highest $\bar{R}^2_{LR}\bar{R}^2_{LR}$ of 0.63 relative to those of Equation 2 ($\bar{R}^2_{LR}$ = 0.62) and Equation 1 ($\bar{R}^2_{LR}$ = 0.43). From this perspective, we can note that DTW combined with FA can predict processes closely related to water movement in the soil, but when more complex factors (i.e., SMR) that integrate additional variables (e.g., soil texture, dynamics of the organic layer, aspect, and primary water source) are modeled, terrain attributes are not sufficient and predictive power decreases.

Conclusions

This study focused on evaluating relationships between site and soil properties relevant to forest management (e.g., SMR, SNR, and drainage regime) and remotely sensed topographic indices (i.e., DTW, FA, and slope), emphasizing the effect of flow initiation area on DTW calculation. The DTW index has the potential for incorporation in site productivity models because it can predict water-related soil attributes. However, it cannot be the only predictor of site productivity because it lacks the ability to characterize other relevant soil properties (e.g., SNR and texture). Furthermore, we explored the limitations of DTW by showing that simple soil attributes (i.e., DtMot) are better predicted by DTW than complex site properties (i.e., SMR), which integrate overall site and soil conditions (e.g., topographic position and texture). The DTW index is currently available for approximately 80% of the forested area of Alberta as well as for areas in the province of New Brunswick and Sweden; thus, our results can directly inform management of forest resources and stimulate research activities. However, because of the complex interactions between the environmental factors controlling soil formation processes, we support the suggestion of Moore et al. (1993) that it is necessary to take a conservative approach when studying the relationships between soil attributes and topographic indices.

Literature Cited

ÅGREN, A.M., W. LIDBERG, M. STRÖMGREN, J. OGILVIE, AND P.A. ARP. 2014. Evaluating digital terrain indices for soil wetness mapping—A Swedish case study. *Hydrol. Earth Syst. Sci.* 18(9):3623–3634.

ALLEN, R.B., R.K. PEET, AND W.L. BAKER. 1991. Gradient analysis of latitudinal variation in Southern Rocky Mountain forests. *J. Biogeogr.* 18(2):123–139.

BECKINGHAM, J.D., AND J.H. ARCHIBALD. 1996. *Field guide to ecosites of northern Alberta.* Northern Forestry Centre, Edmonton, AB, Canada. 336 p.

BEVEN, K.J., AND M.J. KIRKBY. 1979. A physically based, variable contributing area model of basin hydrology. *Hydrol. Sci. Bull.* 24(1):43–69.

BOKALO, M., P.G. COMEAU, AND S.J. TITUS. 2007. Early development of tended mixtures of aspen and spruce in western Canadian boreal forests. *For. Ecol. Manage.* 242(2–3):175–184.

BONTEMPS, J.-D., AND O. BOURIAUD. 2014. Predictive approaches to forest site productivity: Recent trends, challenges and future perspectives. *Forestry* 87(1):109–128.

CAMPBELL, D.M.H., B. WHITE, AND P.A. ARP. 2013. Modeling and mapping soil resistance to penetration and rutting using LiDAR-derived digital elevation data. *J. Soil Water Conserv.* 68(6):460–473.

CHEN, H.Y.H., P.V. KRESTOV, AND K. KLINKA. 2002. Trembling aspen site index in relation to environmental measures of site quality at two spatial scales. *Can. J. For. Res.* 32(1):112–119.

COX, D.R., AND E.J. SNELL. 1989. *The analysis of binary data.* Chapman and Hall, London, UK. 240 p.

DANIEL, T.W., J.A. HELMS, AND F.S. BAKER. 1979. *Principles of silviculture.* McGraw-Hill, New York. 512 p.

GALE, M.R., D.F. GRIGAL, AND R.B. HARDING. 1991. Soil productivity index: Predictions of site quality for white spruce plantations. *Soil Sci. Soc. Am. J.* 55(6):1701–1708.

GESSLER, P.E., O.A. CHADWICK, F. CHAMRAN, L. ALTHOUSE, AND K. HOLMES. 2000. Modeling soil- landscape and ecosystem properties using terrain attributes. *Soil Sci. Soc. Am. J.* 64(6):2046–2056.

HILTZ, D., J. GOULD, B. WHITE, J. OGILVIE, AND P. ARP. 2012. Modeling and mapping vegetation type by soil moisture regime across boreal landscapes. P. 56–75 in *Restoration and reclamation of boreal ecosystems: Attaining sustainable development.* Cambridge Univ. Press, New York.

S Supplementary data are available with this article at http://dx.doi.org/10.5849/forsci.15-054.

IVERSON, L.R., M.E. DALE, C.T. SCOTT, AND A. PRASAD. 1997. A GIS-derived integrated moisture index to predict forest composition and productivity of Ohio forests (USA). *Landsc. Ecol.* 12(5):331–348.

JENNY, H. 1941. *Factors of soil formation: A system of quantitative pedology.* McGraw-Hill, New York. 320 p.

KAYAHARA, G.J., R.E. CARTER, AND K. KLINKA. 1995. Site index of western hemlock (*Tsuga heterophylla*) in relation to soil nutrient and foliar chemical measures. *For. Ecol. Manage.* 74(1–3):161–169.

KAYAHARA, G.J., K. KLINKA, AND A.C. SCHROFF. 1997. The relationship of site index to synoptic estimates of soil moisture and nutrients for western redcedar (*Thuja plicata*) in southern coastal British Columbia. *Northw. Sci.* 71(3):167–173.

KIMMINS, J.P. 2004. *Forest ecology: A foundation for sustainable forest management and environmental ethics in forestry.* Prentice Hall, Upper Saddle River, NJ. 720 p.

KLINKA, K., AND R.E. CARTER. 1990. Relationships between site index and synoptic environmental- factors in immature coastal Douglas-fir stands. *For. Sci.* 36(3):815–830.

KOPECKY, M., AND S. CIZKOVA. 2010. Using topographic wetness index in vegetation ecology: Does the algorithm matter? *Appl. Veg. Sci.* 13(4):450–459.

LANG, M., G. MCCARTY, R. OESTERLING, AND I.Y. YEO. 2013. Topographic metrics for improved mapping of forested wetlands. *Wetlands* 33(1):141–155.

MADDALA, G.S. 1983. *Limited-dependent and qualitative variables in econometrics.* Cambridge Univ. Press, Cambridge, UK. 401 p.

MAGEE, L. 1990. R^2 measures based on Wald and likelihood ratio joint significance tests. *Am. Stat.* 44(3):250–253.

MAILLARD, P., AND T. ALENCAR-SILVA. 2013. A method for delineating riparian forests using region- based image classification and depth-to-water analysis. *Int. J. Remote Sens.* 34(22):7991–8010.

MAJOR, J. 1951. A functional, factorial approach to plant ecology. *Ecology* 32(3):392–412.

MOORE, I.D., P.E. GESSLER, G.A. NIELSEN, AND G.A. PETERSON. 1993. Soil attribute prediction using terrain analysis. *Soil Sci. Soc. Am. J.* 57(2):443–452.

MOORE, I.D., R.B. GRAYSON, AND A.R. LADSON. 1991. Digital terrain modelling: A review of hydrological, geomorphological, and biological applications. *Hydrol. Process.* 5(1):3–30.

MURPHY, P.N.C., J. OGILVIE, AND P. ARP. 2009. Topographic modelling of soil moisture conditions: A comparison and verification of two models. *Eur. J. Soil Sci.* 60(1):94–109.

MURPHY, P.N.C., J. OGILVIE, K. CONNOR, AND P.A. ARPL. 2007. Mapping wetlands: A comparison of two different approaches for New Brunswick, Canada. *Wetlands* 27(4):846–854.

MURPHY, P.N.C., J. OGILVIE, F.R. MENG, B. WHITE, J.S. BHATTI, AND P.A. ARP. 2011. Modelling and mapping topographic variations in forest soils at high resolution: A case study. *Ecol. Model.* 222(14):2314–2332.

NAGELKERKE, N.J.D. 1991. A note on a general definition of the coefficient of determination. *Biometrika* 78(3):691–692.

O'CALLAGHAN, J.F., AND D.M. MARK. 1984. The extraction of drainage networks from digital elevation data. *Comput. Vision Graph.* 28(3):323–344.

PETROSELLI, A., F. VESSELLA, L. CAVAGNUOLO, G. PIOVESAN, AND B. SCHIRONE. 2013. Ecological behavior of *Quercus suber* and *Quercus ilex* inferred by topographic wetness index (TWI). *Trees* 27(5):1201–1215.

PINHEIRO, J.C., AND D.M. BATES. 1995. *Model building for nonlinear mixed-effects models*. University of Wisconsin-Madison, Madison, WI. 11 p.

PINHEIRO, J.C., AND D.M. BATES. 2000. *Mixed-effects models in S and S-PLUS.* Springer-Verlag, New York. 528 p.

PINHEIRO, J.C., D.M. BATES, S. DEBROY, D. SARKAR, AND R CORE TEAM. 2015. *nlme: Linear and nonlinear mixed effects models*. Available online at CRAN.R-project.org/package=nlme; last accessed Apr. 5, 2014.

PITT, D.G., P.G. COMEAU, W.C. PARKER, D. MACISAAC, S. MCPHERSON, M.K. HOEPTING, A. STINSON, AND M. MIHAJLOVICH. 2010. Early vegetation control for the regeneration of a single-cohort, intimate mixture of white spruce and trembling aspen on upland boreal sites. *Can. J. For. Res.* 40(3):549–564.

R CORE TEAM. 2015. *R: A language and environment for statistical computing.* R Foundation for Statistical Computing, Vienna, Austria.

SEIBERT, J., J. STENDAHL, AND R. SORENSEN. 2007 Topographical influences on soil properties in boreal forests. *Geoderma* 141(1–2):139–148.

SORENSEN, R., U. ZINKO, AND J. SEIBERT. 2006. On the calculation of the topographic wetness index: Evaluation of different methods based on field observations. *Hydrol. Earth Syst. Sci.* 10(1):101–112.

TARBOTON, D.G. 1997. A new method for the determination of flow directions and upslope areas in grid digital elevation models. *Water Resour. Res.* 33(2):309–319.

UNG, C.H., P.Y. BERNIER, F. RAULIER, R.A. FOURNIER, M.C. LAMBERT, AND J. REGNIERE. 2001. Biophysical site indices for shade tolerant and intolerant boreal species. *For. Sci.* 47(1):83–95.

WANG, G.G., AND K. KLINKA. 1996. Use of synoptic variables in predicting white spruce site index. *For. Ecol. Manage.* 80(1–3):95–105.

WHITE, B., J. OGILVIE, D.M.H. CAMPBELL, D. HILTZ, B. GAUTHIER, H.K. CHISHOLM, H.K. WEN, P.N.C. MURPHY, AND P.A. ARP. 2012. Using the cartographic depth-to-water index to locate small streams and associated wet areas across landscapes. *Can. Water Resour. J.* 37(4):333–347.

ZIADAT, F.M. 2005. Analyzing digital terrain attributes to predict soil attributes for a relatively large area. *Soil Sci. Soc. Am. J.* 69(5):1590–1599.